First Observation of Hot-Spot Mix in Laser-Direct-Drive Inertial Confinement Fusion

S. P. Regan,[1] V. N. Goncharov,[1] D. Cao,[1] S. X. Hu,[1] I. V. Igumenshchev,[1] R. Epstein,[1] R. Betti,[1] M. J. Bonino,[1] T. J. B. Collins,[1] M. Farrell,[2] C. J. Forrest,[1] V. Gopalaswamy,[1] V. Yu. Glebov,[1] D. R. Harding,[1] R. T. Janezic,[1] J. P. Knauer,[1] R. W. Luo,[2] O. M. Mannion,[1] J. A. Marozas,[1] F. J. Marshall,[1] D. Patel,[1] P. B. Radha,[1] M. E. Schoff,[2] C. Stoeckl,[1] T. C. Sangster,[1] W. Theobald,[1] and E. M. Campbell[1]

[1]Laboratory for Laser Energetics, University of Rochester
[2]General Atomics

A laser-direct-drive (LDD) inertial confinement fusion (ICF) target[1] has spherical concentric layers consisting of a central region of deuterium (D) and tritium (T) vapor surrounded by a cryogenic DT fuel layer and a thin plastic (CH or CD) ablator material. A spherical implosion driven via the rocket effect from laser ablation of the outer target surface by temporally shaped, high-intensity, overlapping laser beams results in the formation of central hot-spot plasma surrounded by a cold, dense DT shell. Thermonuclear fusion (D + T $\rightarrow$ ^{4}He + n) initially occurs in the central hot spot at stagnation, liberating 17.6 MeV per reaction. A long-term goal of ICF is to capture the energy of the alpha particle in the hot spot (i.e., alpha heating) to trigger an ignition instability (i.e., launch a radially outward propagating thermonuclear wave through the surrounding high-density, compressed DT shell), where the fusion energy output is greater than or equal to the laser energy incident on the target. Ignition is predicted to occur when the hot-spot temperature exceeds 5 keV and that compressed areal density exceeds 0.3 g/cm^2 (Refs. 2–4). Perturbations from the target and laser are amplified by the Richtmyer–Meshkov instability (RMI)[5–7] and the Rayleigh–Taylor instability (RTI),[8–10] which could mix the target layers, degrading the implosion compression, enhancing radiative cooling of the hot spot, and reducing the fusion yield and the compressed areal density. Understanding the physical mechanisms and the seeds of hydrodynamic mixing is of great importance to future LDD ICF targets.[11–15]

The amount of hot-spot mix mass in LDD ICF implosions of a plastic spherical shell surrounding a layer of cryogenic DT has been diagnosed for the first time. Layered DT cryogenic implosion experiments were conducted on the 60-beam, 351-nm, 30-kJ OMEGA laser[16] to determine the dependence of hot-spot mix[17–21] on the design adiabat. For the given target dimensions and composition, the adiabat is determined by the time history of the absorbed laser power and the levels of target preheat by either x rays or energetic electrons. The adiabat is defined as the pressure in the compressed shell divided by the Fermi-degenerate pressure at shell density $\left(\alpha = P_{\text{shell}} / P_{\text{Fermi}}\right)$. Evolution of instability seeds due to laser imprint[22] and shell and DT-ice nonuniformities, as well as RTI growth factors during shell acceleration[23] depend on the adiabat; therefore, changing the adiabat varies the hydrodynamic stability of the implosion. Although the OMEGA laser is not energetic enough to ignite a target, it is used to study hydrodynamically scaled ignition target designs.[11–14] The implosion adiabat was varied from 2.5 to 12.5 by adjusting the temporal shape of the laser-drive pulse and the Atwood number at the CH/DT material interface $\left[A_{\text{T}} = \left(\rho_{\text{CH}} - \rho_{\text{DT}}\right) / \left(\rho_{\text{CH}} - \rho_{\text{DT}}\right)\right]$ was varied from –0.14 to +0.04 by changing the amount of x-ray preheat of the ablator from the coronal plasma emission. Hot-spot mix can be seeded by debris or imperfections on the target surface,[17–21,24] engineering features [such as the stalk having a 17-μm outer diameter (OD) or a fill tube with a 10-μm OD],[24] and laser imprint.[22] These seeds are amplified by the RMI during the shock transit of the shell and are subsequently amplified by the RTI of the ablation front and possibly at the CH/DT material interface during the acceleration phase. Additional mixing of the target layers could occur as the converging shell decelerates and forms a central hot spot.

The amount of hot-spot mix mass in LDD ICF implosions of a plastic spherical shell surrounding a layer of cryogenic DT has been quantitatively measured for the first time. Perturbations from the laser and target are amplified by the RMI during the

shock transit of the shell and by the RTI at the ablation surface and the CH/DT material interface during the acceleration phase and the subsequent deceleration phase. The hydrodynamic mixing of material from the plastic ablator, having trace amounts of Ge for diagnosis, into the hot spot at stagnation was observed and quantified using x-ray spectroscopy on the OMEGA laser and was shown to depend on the implosion adiabat and the Atwood number at the CH/DT material interface, consistent with 2-D radiation-hydrodynamic simulations. Hot-spot mix could degrade implosion compression, enhance radiative cooling of the hot spot, and reduce fusion yield and the compressed areal density in future LDD ignition targets.

The inferred hot-spot mix mass versus calculated adiabat is presented in Fig. 1 with (a) showing the case where the RTI at the ablation front and the DT/CH material interface contribute to the hot-spot mix mass, and (b) showing the case where the RTI at the ablation surface is primarily responsible for the hot-spot mix mass. As can be seen in both of these figures, comparable values of mix mass were inferred on each implosion for the two x-ray spectrometers (XRS) used in the experiment: XRS1 (red symbols) and XRS2 (blue symbols). The reduction in the inferred mix mass with increasing adiabat shown in Fig. 1(b) is consistent with the expectation of a decreased level of mixing as the adiabat is increased and the implosion becomes more stable. The weaker dependence of the inferred mix mass on the adiabat and the higher level of inferred mix mass for the highest-adiabat implosion observed in Fig. 1(a) are attributed to additional mixing from instability growth at the unstable DT-ice/plastic ablator interface. The enhanced level of x-ray preheat for the uniformly doped plastic ablator preheats the plastic ablator and causes the DT-ice/plastic ablator interface to become unstable. The trends observed in the experiment are consistent with 2-D radiation-hydrodynamics simulations.

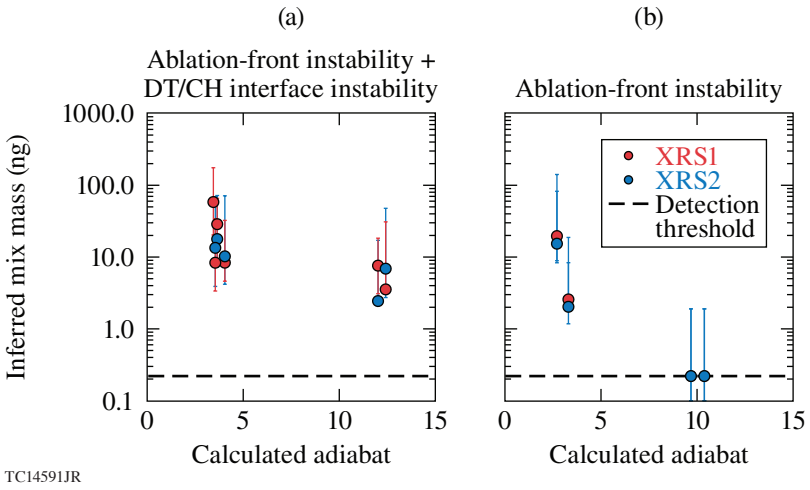

Figure 1
The inferred mix mass for OMEGA DT cryogenic implosions using (a) targets with the 8-μm-thick plastic ablator uniformly doped with Ge, and (b) targets with the inner 3 μm of the 8-μm-thick plastic ablator doped with Ge versus the calculated adiabat. For comparison, the initial CH mass in the shell is 21 μg and the calculated DT mass in the hot spot at stagnation is 1.5 μg.

This material is based upon work supported by the Department of Energy National Nuclear Security Administration under Award Number DE-NA0003856, the University of Rochester, and the New York State Energy Research and Development Authority.

1. J. Nuckolls *et al.*, Nature **239**, 139 (1972).

2. J. D. Lindl *et al.*, Phys. Plasmas **11**, 339 (2004).

3. S. Atzeni and J. Meyer-ter-Vehn, *The Physics of Inertial Fusion: Beam Plasma Interaction, Hydrodynamics, Hot Dense Matter*, 1st ed., International Series of Monographs on Physics, Vol. 125 (Oxford University Press, Oxford, 2004).

4. R. Betti *et al.*, Phys. Plasmas **9**, 2277 (2002).

5. R. D. Richtmyer, Commun. Pure. Appl. Math. **13**, 297 (1960).

6. E. E. Meshkov, Fluid Dyn. **4**, 101 (1969).
7. V. N. Goncharov, Phys. Rev. Lett. **82**, 2091 (1999).
8. J. W. S. Rayleigh, *The Theory of Sound*, 2nd ed., Vol. 2 (Dover, New York, 1945).
9. G. Taylor, Proc. R. Soc. London Ser. A **201**, 192 (1950).
10. A. J. Cole *et al.*, Nature **299**, 329 (1982).
11. V. N. Goncharov *et al.*, Plasma Phys. Control. Fusion **59**, 014008 (2017).
12. E. M. Campbell *et al.*, Matter Radiat. Extremes **2**, 37 (2017).
13. S. P. Regan *et al.*, Nucl. Fusion **59**, 032007 (2019).
14. V. Gopalaswamy *et al.*, Nature **565**, 581 (2019).
15. T. J. B. Collins and J. A. Marozas, Phys. Plasmas **25**, 072706 (2018).
16. T. R. Boehly *et al.*, Opt. Commun. **133**, 495 (1997).
17. B. A. Hammel *et al.*, Phys. Plasmas **18**, 056310 (2011).
18. I. V. Igumenshchev *et al.*, Phys. Plasmas **20**, 082703 (2013).
19. S. P. Regan *et al.*, Phys. Plasmas **19**, 056307 (2012).
20. S. P. Regan *et al.*, Phys. Rev. Lett. **111**, 045001 (2013).
21. R. Epstein *et al.*, AIP Conf. Proc. **1811**, 190004 (2017).
22. V. A. Smalyuk *et al.*, Phys. Rev. Lett. **81**, 5342 (1998).
23. R. Betti *et al.*, Phys. Plasmas **5**, 1446 (1998).
24. T. Ma *et al.*, Phys. Rev. Lett. **111**, 085004 (2013).